Color centers vs electrolytes for Si-based porous anodic alumina

Y.F. Mei [a,*], G.G. Siu [a], J.P. Zou [b], X.L. Wu [b]

[a] *Department of Physics and Materials Science, City University of Hong Kong, Kowloon, Hong Kong, PR China*
[b] *National Laboratory of Solid State Microstructures and Department of Physics, Nanjing University, Nanjing 210093, PR China*

Abstract

Anodic oxidation of Al film on silicon substrate in three different electrolytes is investigated through j–t curves and photoluminescence (PL) of the grown porous anodic alumina (PAA) under same voltage. Their growth is analyzed with three typical stages according to j–t curve. The influence of the electrolyte on color centers is shown through comparison of the PL spectra of Si-based PAA fabricated in different electrolytes. From sulfuric, oxalic to phosphoric acids, The PL shows blueshift behavior with different electrolytes due to mechanical stress and concentration of defect centers, while the change of PL intensity reduced for decreasing of the contrast across barrier layer, which is helpful to understand PL mechanism and growth mechanism of porous anodic alumina.
© 2004 Elsevier B.V. All rights reserved.

PACS: 78.55.-m; 78.55.Mb; 61.72.Ji; 82.80.Fk

Keywords: Photoluminescence; Porous materials; Color centers; Electrochemical methods

1. Introduction

Porous anodic alumina (PAA), a porous oxide membrane formed on aluminum, is very useful as template in fabrication of nanomaterials and nanostructures [1–3], such as carbon nanotube (CNT) [4], monocrystal Ag nanowires [5], and CdS nanowires [6]. Nanostructures and their array are synthesized on various substrates with PAA template such as Si substrate [7–9] for nanoelectrics, on glass substrate with a conductive tin doped indium oxide layer [10] for display and on thin film such as SiGe [11] or SiO_2 [12] on silicon substrate for nanooptoelectronics. Experimental and theoretical progress has been made to elucidate anodization of PAA, important for improving nanostructure fabrication, especially when PAA template is converted to other substrate.

The properties of PAA are affected by many anodization variables (e.g., voltage, temperature, and electrolyte concentration). Among its properties, the optical one not only characterizes PAA itself but also decides its potential application in light source array [12] and nanolaser [13], etc. PAA can emit light when excited with UV radiation. This photoluminescence (PL) is susceptible to its environment because of its porous structure and amorphous morphology [14]. PL was attributed some impurity at first [15]. Recently the singly ionized oxygen vacancies (F^+ center) were sug-

* Corresponding author.
  E-mail address: meiyongfeng@nju.org.cn (Y.F. Mei).

gested as PL centers through electron paramagnetic resonance (EPR) [16]. Analyses of PL peaks showed that there are two different defects (F and F^+ centers) in PAA [17]. The asymmetry of PL bands was attributed to the inhomogeneity in defect distribution. However, for the identified PL mechanism of PAA, it is necessary to reveal the details of growth condition of PAA and its relationship with optical property.

In this work, Si-based PAA are prepared electrochemically in different electrolytes. Their growth is monitored through the dependence of current density on time (j–t curves) and PL, showing defect (color center) variations corresponding to different electrolyte. The PL shift with different electrolytes was due to mechanical stress and concentration of defect centers, while the change of PL intensity was related to the E-field contrast across the barrier layer.

2. Experiments

Aluminum film (99.99%) with thickness 440 nm was deposited on the p-type, 0.5 Ω cm, and $\langle 100 \rangle$-oriented silicon substrate using electron beam evaporation. The vacuum chamber was maintained under a pressure of 2.5×10^{-6} Pa. The accelerating voltage of the electron beam is held essentially constant ~ 10 kV and electron gun current is 0.5 A. As-deposited Al film had smooth and compact surface, and Al film on Si substrate (Al/Si) was directly used as an anode with a platinum plate as a cathode. Several Al/Si were anodized in aqueous solution of 15 wt.% sulfuric acid, 0.5 M oxalic acid, and 0.87 M phosphoric acid under a constant DC voltage of 40 V at room temperature. The growth process can be monitored with j–t curves. The surface of the fabricated PAA was checked by a JEOL JSM-6300 scanning electron microscope (SEM), and PL was measured at room temperature by a FluoroMax-2 photospectrometer.

3. Results and discussion

Fig. 1 shows the j–t curves for anodization of Si-based PAA respectively in the acid solutions of: (a) 15 wt.% sulfuric acid (as [8]), (b) 0.5 M oxalic acid, and (c) 0.87 M phosphoric acid (as [17]) at room temperature. In Fig. 1(b), typical stages are included
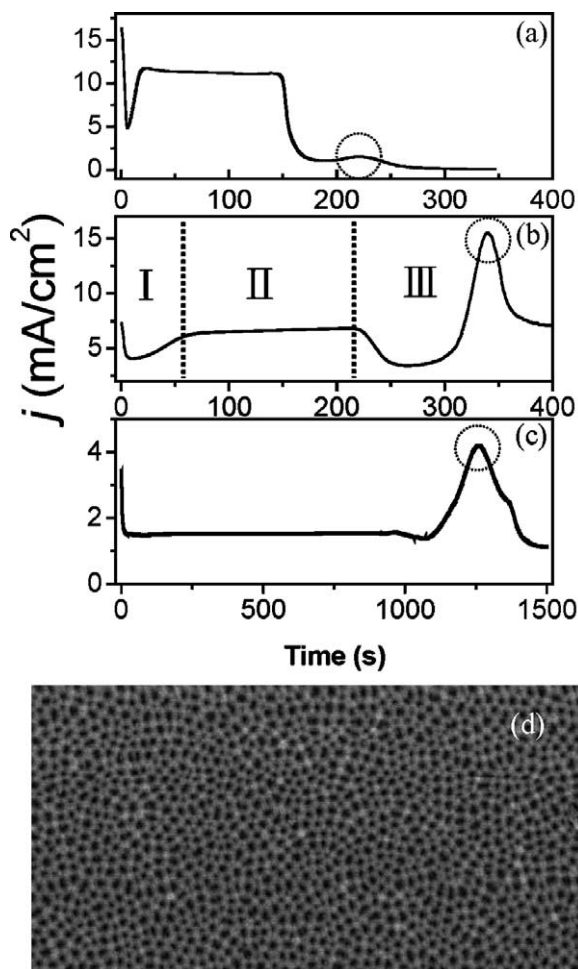

Fig. 1. The j–t curves for anodization of Si-based PAA film in (a) 15 wt.% sulfuric acid, (b) 0.5 M oxalic acid, and (c) 0.87 M phosphoric acid under DC voltage 40 V at room temperature, (d) is the planar SEM image of PAA template on silicon substrate formed in oxalic acid.

by three anodization processes, corresponding to (I) the initiation of nanopores, (II) the stable growth of channels in Si-based PAA, (III) and the transition of anodization from aluminum film to silicon substrate.

According to the existing point of view, anodization processes from aluminum to silicon substrate. In stage I immediately after switching on the anodic bias, the current density (j) decreases for the existence of natural thin oxide layer on the aluminum film. When the natural oxide layer is eat off, the current density increases and reaches a stable anodization in stage II, when oxide growth and dissolution are balanced.

Table 1
The parameters of Si-based PAA films formed in different acid solutions

Solution	Sulfuric acid	Oxalic acid	Phosphoric acid
Concentration	15 wt.%	0.5 M	0.87 M
DC voltage	40 V	40 V	40 V
Pore diameter	25 nm	50 nm	80 nm
Interpore diameter	50 nm	75 nm	110 nm
Pore density	4.62×10^{10} cm^{-2}	2.05×10^{10} cm^{-2}	9.54×10^{9} cm^{-2}
Current density	14.4 mA cm^{-2}	6.56 mA cm^{-2}	1.44 mA cm^{-2}

When aluminum is going to be exhausted, the current density declines at the beginning of stage III because anodization of silicon substrate starts at the same time. In stage III, the alumina dissolution reduces resistance since no more oxide growth without residual Al [19]. Silicon oxide formed in the anodization of silicon substrate, on the contrary, increases the resistance of substrate. The competition of the two generates a minimum in the surface resistance, which increases later. Correspondingly the current density reaches a maximum at the position C (the dotted circle in Fig. 1(b)). The anodization in three electrolytes is similar as shown in Fig. 1(a) and (c).

The SEM image of the sample anodized in 0.5 M oxalic acid solution is shown in Fig. 1(d). A uniform nanopores array can be observed. Owing to small grain (100–1000 nm) [9], their arrangement has lower order than PAA on bulk Al [2]. With similar condition, Si-based PAA films are fabricated in 15 wt.% sulfuric acid [9] and 0.87 M phosphoric acid [18] under the same DC voltage (see in Table 1). Different pore size can be formed because part of the voltage is added onto the silicon substrate [20]. Different features are shown in Table 1 for Si-based PAA formed in different acids.

There is a maximum (the dotted circles) of j in all three electrolytes, which needs different anodization time. Estimated from this time, the anodization speed v is the fastest in sulfuric acid and the slowest in phosphoric acid, despite the same thickness of Al film on silicon substrate and the same DC voltage. That is, qualitatively, $v_s > v_o > v_p$ (s, o, p denote sulfuric, oxalic, and phosphoric acids, respectively). It is related to different thickness of the formed barrier layer [21] and different anodization speed for aluminum and silicon [9] in different electrolytes. The steady current densities of anodization in different electrolytes are different owing to different electrolyte conductivity [17].
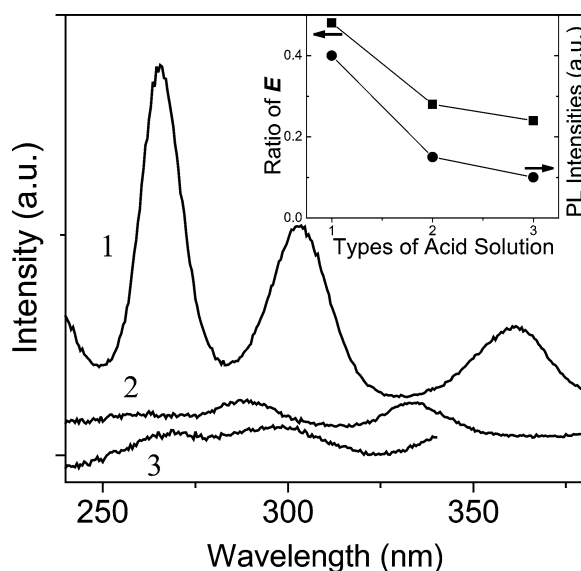

Fig. 2. The PL spectra of Si-based PAA films formed in different acid solutions, 1: 15 wt.% sulfuric acid, 2: oxalic acid, 3: phosphoric acid; the inset shows the relationship between PL intensities and the ratio of E for PAA films in different acid.

It is interesting to know whether there is any difference in the defects in the three samples. Fig. 2 shows the PL spectra of completely grown Si-based PAA film in different acid solution. Different excitation wavelengths were adopted in order to get the maximal PL intensity for every sample. So the excitation wavelengths for Si-based PAA formed in sulfuric acid, oxalic acid, and phosphoric acid are respectively 220, 200, and 190 nm, which can be suggested corresponding to the band energy level in alumina (220 nm) [22]. The inset shows the intensity variation, which manifest the influence of different electrolytes on defects. The defects were suggested as color centers (F and F^{+}) as previous work [14,17].

These peaks in three samples also show blueshifts from sulfuric acid to phosphoric acid. Mechanical stress is an important factor to affect the shift for anodization in different electrolytes. Increasing stress causes redshift due to the increase of wavefunction overlap, i.e., the decreasing of the spacings of the energy levels of the defect centers. When aluminum is oxidized to alumina, the volume expands by roughly a factor of 2 because the atomic density of aluminum in alumina is a factor of 2 lower than in metallic aluminum [23]. The rate of volume expansion, which leads to compressive stress in the film, is proportional to the anodization speed. It can be deduced that the stress σ in PAA film is $\sigma_s > \sigma_o > \sigma_p$ owing to $\nu_s > \nu_o > \nu_p$. Hence the blueshifts happen in these three samples fabricated in different electrolytes. However, a redshift can be caused by an increase of oxygen vacancies in PAA film [16] and silica [24]. As the following explanation, the defect densities n in three samples are $n_s > n_o > n_p$, which can also induce blueshifts. It is difficult to ascertain which of the two mechanisms predominates.

For PL intensity variation with samples, why are they different with different acid? The intensities of their PL excitation (PLE) agree with PL intensities. So the non-radiation of defects can be ignored. We assume that the concentration of defect centers should be responsible for the change of PL intensities. More defect centers, stronger PL peaks. The inhomogeneous distribution of defects may be explained using non-linear gradient of electric field across the barrier layer, because the incorporations of oxygen anions and the formation of defects centers from oxygen anions become pronounced due to the large contrast of E-field at two ends of the barrier layer [25]. As shown in Fig. 3 [25], the electric field strength, E, should increase between the cell base (wx) and the pore base (yz) [26]. The field strength in the barrier layer can be estimated using the following equation [27].

$$j = j_0 \exp\left[-(w - qaE)/kT\right], \qquad (1)$$

where $j_0 = 2.24 \times 10^7 \ \mathrm{A\,cm^{-2}}$, $w = 1.3 \ \mathrm{eV}$, $q = 3 \ \mathrm{e}$, $a = 2.95 \ \text{Å}$.

Substituting the parameters from Table 1, we can estimate the E-fields at the cell base and the pore base with different templates. The fields at the pore base are larger by 4.8%, 2.8%, and 2.4% than that at cell base in Si-based PAA films formed in sulfuric,
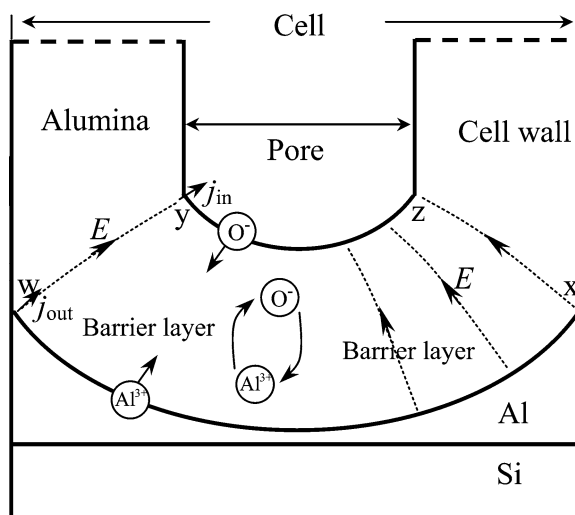

Fig. 3. The schematic diagram for explanation of the non-linear gradient of the electric field across the barrier layer of Si-based PAA film.

oxalic, and phosphoric acids, respectively. The E-field ratio on the two sides of barrier layer is now compared with the variation of PL intensity, they agree well (see the inset in Fig. 2). It shows that higher contrast of the E-field across barrier layer induces more defect concentration (i.e., stronger PL), which is helpful to understand the growth mechanism of PAA.

4. Conclusion

Anodic oxidation of Al film on silicon substrate under same voltage in three different electrolytes is investigated through the j–t curves and the PL of the grown PAA. Their growth processes are generally included by three typical stages. From sulfuric, oxalic to phosphoric acids, the concentration of color centers decreases. The PL spectra show the electrolyte influence on color centers through stress effect and E-field contrast effect, which is helpful to understand PL mechanism and growth mechanism of PAA.

Acknowledgements

References

[1] R. Parthasarathy, C.R. Martin, Nature 369 (1994) 298.
[2] H. Masuda, K.S. Fukuda, Science 268 (1995) 1466.
[3] S. Shingubara, J. Nanoparticle Res. 5 (2003) 17.
[4] J. Li, C. Papadopoulos, J.M. Xu, Nature 402 (1999) 253;
    J. Sang, J.S. Lee, Appl. Phys. Lett. 75 (1999) 2047.
[5] J. Zhang, X. Wang, X. Peng, L. Zhang, Appl. Phys. A 75 (2002) 485.
[6] D. Routkevitch, T. Bigioni, M. Moskovits, J.M. Xu, J. Phys. Chem. 100 (1996) 14037;
    H.Q. Cao, Y. Xu, J.M. Hong, H.B. Liu, G. Yin, B.L. Li, C.Y. Tie, Z. Xu, Adv. Mater. 13 (2001) 1393.
[7] H. Masuda, K. Yasui, Y. Sakamoto, M. Nakao, T. Tamamura, K. Nishio, Jpn. J. Appl. Phys. 40 (2001) L1267;
    S. Shingubara, O. Okino, Y. Sayama, H. Sakaue, T. Takahagi, Solid State Electron. 43 (1999) 1143.
[8] W.C. Hu, D.W. Gong, Z. Chen, L.M. Yuan, K. Saito, C.A. Grimes, P. Kichambare, Appl. Phys. Lett. 79 (2001) 3083.
[9] Y.F. Mei, X.L. Wu, X.F. Shao, G.S. Huang, G.G. Siu, Phys. Lett. A 309 (2003) 109.
[10] S.Z. Chu, K. Wada, S. Inoue, S.I. Todoroki, Chem. Mater. 14 (2002) 266.
[11] J. Rappich, Solid State Electron. 45 (2001) 1465.
[12] J.P. Zou, Y.F. Mei, J.K. Shen, J.H. Wu, X.L. Wu, X.M. Bao, Phys. Lett. A 301 (2002) 96.
[13] X.F. Duan, Y. Huang, R. Agarwal, C.M. Lieber, Nature 421 (2003) 241.
[14] J.H. Wu, X.L. Wu, N. Tang, Y.F. Mei, X.M. Bao, Appl. Phys. A 72 (2001) 735.
[15] Y. Yamamto, N. Baba, S. Tajima, Nature 289 (1981) 572.
[16] Y. Du, W.L. Cai, C.M. Mo, J. Chen, L.D. Zhang, X.G. Zhu, Appl. Phys. Lett. 74 (1999) 2951.
[17] G.S. Huang, X.L. Wu, Y.F. Mei, X.F. Shao, G.G. Siu, J. Appl. Phys. 93 (2003) 582.
[18] Y. Yang, H.L. Chen, Y.F. Mei, J.B. Chen, X.L. Wu, X.M. Bao, Acta Mater. 50 (2002) 5085;
    Y. Yang, H.L. Chen, Y.F. Mei, J.B. Chen, X.L. Wu, X.M. Bao, Solid State Commun. 123 (2002) 279.
[19] N. Kouklin, L. Menon, A.Z. Wong, D.W. Thompson, J.A. Woollam, P.F. Williams, S. Bandyopadhyay, Appl. Phys. Lett. 79 (2001) 4423.
[20] Y.F. Mei, X.L. Wu, X.F. Shao, G.G. Siu, X.M. Bao, Europhys. Lett. 62 (2003) 595.
[21] G.E. Thompson, G.C. Wood, Nature 290 (1981) 230.
[22] Y.L. Shi, J. Wang, H.L. Li, Appl. Phys. A 75 (2002) 423.
[23] O. Jessensky, F. Müller, U. Gösele, Appl. Phys. Lett. 72 (1998) 1183.
[24] H.R. Philipp, J. Phys. Chem. Solids 32 (1971) 1935.
[25] V.P. Parkhutik, V.I. Shershulsky, J. Phys. D 25 (1992) 1258.
[26] T.P. Hoar, N.F. Mott, J. Phys. Chem. Solids 9 (1959) 97.
[27] A.C. Harkness, L.C. Young, J. Chem. 44 (1966) 2409.